

## Influence of the first wall material on particle fuelling

E. Wolfrum<sup>1</sup>, T. Lunt<sup>1</sup>, F. Reimold<sup>2</sup> and the ASDEX Upgrade Team

*1 Max-Planck-Institute for Plasma Physics, 85748 Garching, Germany*

*2 Institut für Energie und Klimaforschung – Plasmaphysik, Forschungszentrum Jülich,  
52425 Jülich, Germany*

In the past carbon was preferentially chosen as first wall material for tokamaks, as high  $Z$  materials can radiate significant power fractions in the confined region thereby cooling the plasma. However, carbon is not a viable first wall material for a reactor, because of the large co-deposition of deuterium and tritium in carbon plasma facing components (PFCs), which would soon exceed the permitted limits for the radioactive tritium inventory. In ASDEX Upgrade the graphite and CFC (carbon fiber reinforced carbon) first wall tiles were therefore gradually replaced by tungsten (W) coated PFCs in the period from 2003 to 2007 [1].

The most important properties of the W-PFCs are the reduced D retention [2] as well as the higher threshold for physical sputtering [3]. Contributing to this effect is on the one hand the reduced chemical reactivity of W as compared to C, but also the higher reflection coefficient. Ions incident on a PFC can be scattered or adsorbed at a surface. The reflection coefficients defined in [4] provide a measure of the amount of reflected particles and their energy with respect to the incident flux of particles and energy. Following reference [4] the sum over all escaping atoms with different emission energies, angles and charge states is denoted the particle (number) reflection coefficient  $R_N$ . Integration over the emission energies and angles of all reflected particles gives the energy reflection coefficient  $R_E$ . The mean energy  $\langle E \rangle$  of reflected atoms can be determined by  $\langle E \rangle = E_0 \cdot R_E / R_N$ , where  $E_0$  is the energy of the incident atom or ion. Table 1 shows the values of  $R_N$ ,  $R_E$  and  $\langle E \rangle$  for deuterium incident on C and W, for the incident energies 10, 20 and 50 eV according to Ref.[4].

E <sub>0</sub>	D → C			D → W		
	R <sub>N</sub>	R <sub>E</sub>	$\langle E \rangle$	R <sub>N</sub>	R <sub>E</sub>	$\langle E \rangle$
10 eV	0.4	0.13	2.5 eV	0.8	0.6	7.5 eV
20 eV	0.32	0.12	7.5 eV	0.71	0.52	14.6 eV
50 eV	0.3	0.1	16.6 eV	0.68	0.38	27.9 eV

Table 1. Particle and energy reflection coefficients,  $R_N$  and  $R_E$ , as well as mean energies  $\langle E \rangle$  for D ions incident on C or W for three selected incident energies  $E_0$ .

As can be seen from table 1, not only the probability to be reflected from W is higher by a factor of 2 for a 10 eV incident D ion, but also the mean energy of the reflected atom is 7.5 eV, which is 3 times higher than the mean energy of a 10 eV ion reflected from C.

This higher reflection coefficient leads to a large fraction of neutrals, which are not thermally recycled from the wall, but which are reflected, i.e. incident ions are neutralized upon wall contact and directly repelled back into the plasma. While thermally recycled neutrals have energies  $< 1$  eV, the reflected neutrals can carry a large fraction of the energy of the incident ions, i.e. between 5 and 30 eV. Such high energy neutrals have longer mean free paths and the probability that they are ionized in the confined plasma is higher than that of low-energetic neutrals. They form a local source and can change the shape of the edge density profile.

In the following we present edge electron density ( $n_e$ ) profiles of discharges conducted in ASDEX Upgrade with the full W-PFCs coverage and compare them to profiles acquired in very similar discharges with C-PFCs. The electron density profiles are acquired with the Lithium beam emission spectroscopy diagnostic (Li-BES) [5] and have a temporal resolution of 1 ms.

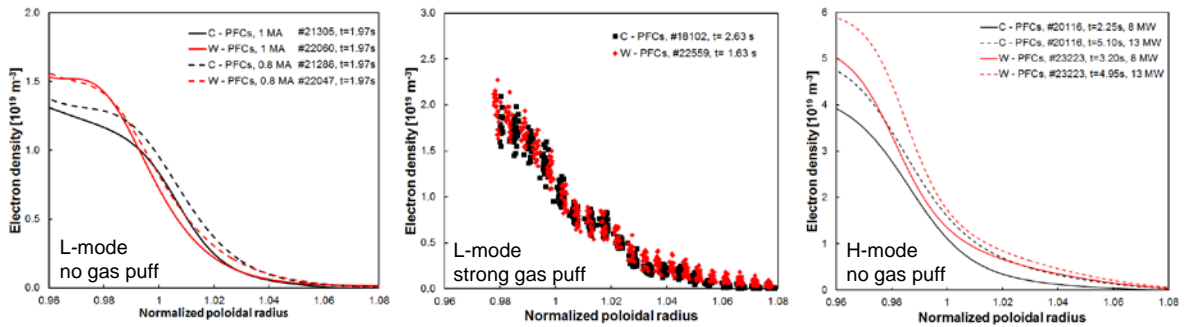


Figure 1: Density profiles before and after the change from a C (black) to a W (red) wall. a) L-modes without gas puff at two currents,  $I_p = 800$  kA (dashed lines) and 1 MA (solid lines). b) L-mode with strong gas puff. c) H-modes without gas puff at two different heating powers, 8 MW (solid lines) and 13 MW (dashed lines).

The first two examples, shown in figure 1a, are edge  $n_e$  profiles in low confinement mode (L-mode) at two different plasma currents,  $I_p = 0.8$  and 1 MA, at magnetic fields  $|B_t| = 2 - 2.2$  T, with no gas puffing. Although the relative positioning could change due to uncertainties in the diagnostic and the equilibrium, it is obvious that the edge  $n_e$  profiles in the C-PFC cases show lower values at  $\rho_{pol} = 0.98$  for both plasma currents. Moreover, the gradients, averaged in the steep gradient region, are stronger in the W-PFC cases. It is important to note that these profiles are established with no gas puffing. As the gas puffing is increased,  $n_e$  in the scrape-off layer (SOL) rises and the divertor becomes more and more collisional. The collisionality in the divertor can lead to the formation of larger filaments which move across the SOL [6]

and contribute to the density profile in the form of a shoulder, i.e. a region with very long decay length. In figure 1b two of such L-mode profiles are compared, again one with W and one with C-PFCs. Both discharges are ohmically heated, with  $I_p = 800$  kA and  $|B_t| = 2.5$ T. All available  $n_e$  profiles during a 40 ms period are plotted. In this case no difference in the density profiles can be seen. Finally, in figure 1c we present examples of H-mode profiles from phases of similar discharges with the two different wall materials without gas puffing. The discharges and profiles have been described earlier [7]. They stem from discharges with  $I_p = 1$  MA,  $|B_t| = 2.5$  T, and have phases with different heating power. Only profiles from the period -3 ms to -1 ms before an ELM are selected in a 300 ms phase with otherwise constant plasma parameters. In both heating power cases the  $n_e$  profiles with W-PFCs reach higher pedestal top values. As was shown in reference [7], the electron temperature ( $T_e$ ) at the pedestal top is lower in W wall, leading to similar edge pressure profiles for these cases, indicating that the boundary for peeling-ballooning (PB) stability has not changed. In summary, the profiles without gas puff and otherwise similar discharge parameters and for the H-mode cases at the same PB stability boundary have in common that they show higher pedestal top densities, while the L-mode discharge with a dense SOL does not show this effect. In strongly gas puffed H-modes several other effects influence the density profile [8], and they are not considered here.

The neutral particle and plasma transport was also studied by means of EMC3-Eirene simulations. EMC3 solves Braginskii-like equations treating the plasma as a fluid and is self consistently coupled to Eirene [9] that simulates the neutral particle transport kinetically. The details of EMC3 and the coupling of the two codes is described in [10]. We assumed a density at the separatrix of  $n_{e,sep} = 8 \cdot 10^{18} \text{ m}^{-3}$  and an input power  $P_{in} = 800$  kW equally distributed between the ions and the electrons. Furthermore, diffusive transport coefficients  $D_{\perp} = 0.1 \text{ m}^2/\text{s}$  in the core to  $D_{\perp} = 0.9 \text{ m}^2/\text{s}$  in the SOL, with  $\chi_{\perp} = 3D_{\perp}$  are assumed to emulate a low-power, low-density L-mode discharge. For particles the computational domain is a closed system, the only neutral particle sources are the PFCs, where recycling occurs. Figure 2 shows radial profiles of  $n_e$ ,  $T_e$  and the ionization profile  $S_i$  predicted by EMC3-EIRENE with the assumed transport coefficients for C and W as wall material, as well as for C where the particles recycle only thermally, i.e.  $R_{fast}$  is set to 0. While  $n_e$ ,  $T_e$  and  $D_{\perp}$  are given along a straight line at the outboard midplane,  $S_i$  is poloidally averaged in the confined region. The profiles show a significant dependence on the wall material, which is attributed to the enhanced reflection from the tungsten walls. In these cases, the contribution from the divertor region is dominant.

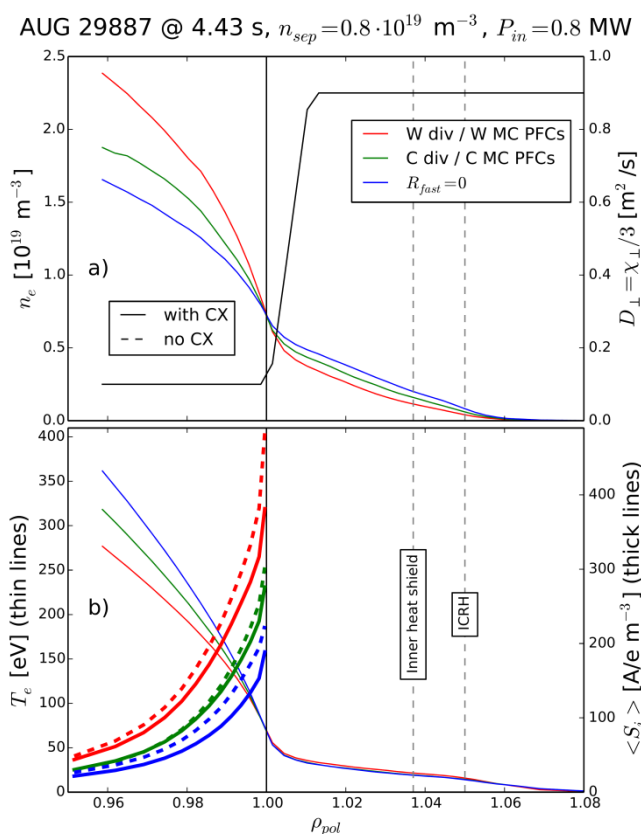


Figure 2: a) Midplane  $n_e$  profiles calculated with EMC3-Eirene for W-PFCs (red), C-PFCs (green) and C-PFCs without fast reflected neutrals (blue) as well as transport coefficients (black).  
b) Midplane  $T_e$  profiles and poloidally averaged ionisation profiles.

For higher densities, however, recycling on the main chamber PFCs has a larger contribution. As the density is increased even further, the impact of the directly reflected neutrals on the profiles becomes smaller, because ion temperature and therefore the energy of the neutrals at the target is smaller and the SOL more opaque, see the example in figure 1b, where most recycled neutrals are ionised in the SOL and do not contribute to the pedestal top density. In summary, evidence is given that in plasmas with low density scrape-off layers, which are highly transparent for neutrals, the effect of higher particle and energy reflection from the W wall leads to steeper edge density profiles as well as higher pedestal top densities in ASDEX Upgrade. For experiments with strong gas puffing the divertor and the

SOL is more opaque to neutrals and additional effects can become important [11].

#### Acknowledgements:

This work has been carried out within the framework of the EUROfusion Consortium and has received funding from the Euratom research and training programme 2014-2018 under grant agreement No 633053. The views and opinions expressed herein do not necessarily reflect those of the European Commission.

#### References:

- [1] R. Neu et al., J. Nucl. Mat. 367 (2007) 1497-1502
- [2] V. Rohde et al., Nucl. Fusion 49 (2009) 085031 (9pp)
- [3] A. Kallenbach et al., J. Nucl. Mat. 415 (2011) S19-S26
- [4] W. Eckstein, Report IPP 17/12, IPP Garching 2009
- [5] M. Willensdorfer et al., Plasma Phys. Control. Fusion 56 (2014) 025008
- [6] D. Carralero et al., Phys. Rev. Lett. 115 (2015) 215002
- [7] P.A. Schneider et al., Plasma Phys. Control. Fusion 57 (2015) 014029
- [8] M. Dunne et al., this conference
- [9] D. Reiter et al., J. Nucl. Mat. 196-198 (1992) 1059-1064
- [10] Y. Feng et al., Contrib. Plasma Phys. 54 (2014) 426
- [11] F. Reimold et al., PSI 2016